



# The University of Bradford Institutional Repository

<http://bradscholars.brad.ac.uk>

This work is made available online in accordance with publisher policies. Please refer to the repository record for this item and our Policy Document available from the repository home page for further information.

To see the final version of this work please visit the publisher's website. Available access to the published online version may require a subscription.

Link to original published version: <http://doi.org/10.1680/stbu.2003.156.4.395>

Citation: El-Refaie, S. A., Ashour, A. F. and Garrity, S. W. (2003) CFRP strengthened continuous concrete beams. Proceedings of the Institution of Civil Engineers - Structures and Buildings, 156 (4): 395-404.

Copyright statement: © 2003 ICE. Reproduced in accordance with the publisher's self-archiving policy.



# **THE USE OF EXTERNAL CFRP FOR CONTINUOUS CONCRETE BEAMS: A PRELIMINARY INVESTIGATION**

by

**S. A. El-Refaie, A. F. Ashour\* and S. W. Garrity**

## **ABSTRACT**

This paper reports the testing of five reinforced concrete continuous beams strengthened in flexure with externally bonded carbon fibre reinforced polymer (CFRP) laminates. All beams had the same geometrical dimensions and internal steel reinforcement. The main parameters studied were the position and form of the CFRP laminates. Three of the beams were strengthened using different arrangements of CFRP plate reinforcement and one was strengthened using CFRP sheets. The performance of the CFRP strengthened beams was compared with that of an unstrengthened control beam. Peeling failure was the dominant mode of failure for all the strengthened beams tested. The beam strengthened with both top and bottom CFRP plates produced the highest load capacity. It was found that the longitudinal elastic shear stresses at the adhesive/concrete interface calculated at beam failure were close to the limiting value recommended in the Concrete Society Technical Report 55.

## **INTRODUCTION**

Bonding plate reinforcement to the external surfaces of existing reinforced concrete elements has proved to be an effective and a practical means of increasing strength and

---

\* Corresponding author

stiffness. Recently, fibre reinforced polymer (FRP) composite plates have been used as an alternative to steel. FRP composites have many advantages over steel plates including a high strength to weight ratio, corrosion resistance, availability in greater lengths and ease of handling. FRP composites, however, are costly and have no ductility that could lead to undesirable brittle failure of the strengthened elements.

Although several research studies have been conducted on the strengthening and repair of simply supported reinforced concrete beams using external plates<sup>1-7</sup>, there is little reported work on the behaviour of strengthened continuous beams<sup>8-10</sup>. The authors<sup>8</sup> previously tested a series of two span reinforced concrete beams with external CFRP sheets. It was found that increasing the length and number of CFRP layers produced a higher load capacity up to a certain limit beyond which no further improvement could be achieved. Overall, the beam ductility was reduced. This paper summarises the testing of a second series of continuous beams with externally bonded CFRP plates and sheets. Unlike the previous tests by the authors, the top steel reinforcement over the central support is the same as that provided at the mid-spans and both hogging and sagging regions were strengthened with CFRP laminates. The principal aims of this paper may be summarised as follows:

- To study the effectiveness of strengthening continuous reinforced concrete beams using CFRP laminates. Three measures are considered for this purpose, namely ultimate load enhancement ratio, moment enhancement ratio and ductility;
- To examine different modes of failure of continuous beams strengthened with CFRP laminates;
- To compare the performance of continuous beams strengthened with CFRP sheets and plates of equivalent strength;

- To compare the longitudinal elastic shear stresses between the adhesive/concrete interface at the beam failure with the limiting values suggested by other researchers.

## **TEST PROGRAMME**

Five large scale reinforced concrete two span beams, hereafter referred to as E1 to E5, were tested to failure. The beam geometry and reinforcement, as well as the loading and support arrangement are illustrated in Figure 1. Each beam was 8500mm long x 150mm wide x 250mm deep. The longitudinal reinforcement consisting of four 16mm diameter bars was the same in each beam. These bars were not curtailed in order to simplify construction. Vertical links of 6mm diameter spaced at 100mm centres along each beam were provided to prevent shear failure.

The position and form of the CFRP laminates were the main parameters investigated, as summarised in Table 1. The laminates applied to the top face of the beams were 2500mm long and were placed symmetrically about the line of the central support. A 2500mm length of CFRP was used to ensure that the external reinforcement extended past the point of contra-flexure in all tests. Those applied to the bottom face of the beam were 3500mm long and were positioned symmetrically about the centres of both spans. The CFRP laminate length was chosen to cover the entire hogging zone for beams strengthened over the central support and the entire sagging zone in case of soffit plated beams. The purpose of this selection is to reduce the stress concentration at the plate ends and hence to prevent the initiation of peeling failure of the CFRP laminates. Beam E1 had no external reinforcement and was used as a control specimen. The top of the central region of beam E5 was strengthened with CFRP sheets (6 layers of 0.702mm total thickness x 110mm wide x 2500mm long) of the same tensile strength as that of the CFRP plates used for beams E2, E3 and E4.

## MATERIAL PROPERTIES

The beams were made from Ordinary Portland cement with a 10mm maximum aggregate size and a target 28 day compressive strength of 30 N/mm<sup>2</sup>. For each batch of concrete made to manufacture the test beams, three 100mm cubes and three 100x100x500mm prisms were produced. The cubes and prisms were tested on the same day as the test beams to provide values of the cube strength  $f_{cu}$  and the modulus of rupture  $f_r$ . The average values of  $f_{cu}$  and  $f_r$  together with the yield strength  $f_y$  and modulus of elasticity  $E_s$  of the steel reinforcement are given in Table 2.

## STRENGTHENING PROCESS

The unidirectional CFRP sheets, pultruded CFRP plates, epoxy primer and epoxy bonding and structural adhesives were provided by Weber and Broutin (UK) Ltd; details of the mechanical properties of these strengthening materials, taken from the manufacturer's data sheets, are summarised in Table 3. The CFRP plates were manufactured using the pultrusion process and have a fibre volumetric content of 70% in an epoxy resin matrix. The CFRP sheets were not pre-impregnated with epoxy resin; i.e. they were only dry carbon fibre. When they are formed into a laminate, the resulting effective properties will be lower than those given in Table 3 for dry CFRP sheets. Both the CFRP sheets and plates were uni-directional fibres in the longitudinal direction.

### ***Surface preparation***

In order to expose the aggregate, the concrete substrate of the beam was initially roughened by sand blasting and then vacuum cleaned to remove any dust or loose particles. A 300mm straight edge was used to check that the surface deviation was within the acceptable 1mm limit recommended by the manufacturer. The quality of the prepared concrete substrate was assessed by carrying out a pull-off bond test in accordance with

the BS1881 (1992)<sup>16</sup>. The pull-off bond strength was compared with the manufacturer's following recommendations: at least 1.0 N/mm<sup>2</sup> for applying CFRP sheets and 1.5 N/mm<sup>2</sup> for applying CFRP plates. The CFRP plates and sheets were then applied using the appropriate bonding adhesive in accordance with the manufacturer's instructions as explained below.

### ***Installing the CFRP plates***

A two-component epoxy resin structural adhesive was prepared in accordance with the manufacturer's recommendations giving a soft paste like consistency when mixed. The structural adhesive was applied by trowel on both the clean CFRP plate (protected by a peel-off strip) and the prepared concrete surface separately. Then, the CFRP plate was placed immediately on the concrete substrate and pressed with a rubber roller. The thickness of the structural adhesive layer was 3.0mm, as advised by the material supplier.

### ***Installing the CFRP sheets***

Two-component epoxy resin primer was prepared in accordance with the manufacturer's recommendations and applied to the concrete substrate by brush. When the primer had dried to a touch-dry state, two-component epoxy resin bonding adhesive was prepared in accordance with the manufacturer's recommendations and applied by brush over the touch-dry primer. The first layer of CFRP sheet was then placed by hand and pressed onto the adhesive with a rubber roller. Another layer of adhesive was applied over the CFRP sheet and was dispersed using a squeegee. Additional CFRP layers were applied in the same way onto the uncured wet adhesive.

## **TEST RIG**

After bonding the external CFRP laminates, the complete application was subsequently left to cure for at least 7 days before beam testing. Each test beam, which comprised two

equal spans of 3830mm each, was loaded as shown in Figure 1. Load cells were used to measure the end support reactions and electrical resistance strain (ERS) gauges were attached to the longitudinal steel bars and CFRP laminates at the bottom mid-spans and the top over the central support to measure surface strains. The mid-span deflections were measured using linear variable differential transformers (LVDTs). Load cell, ERS gauge and LVDT readings were recorded automatically, at each increment of the applied load (10 kN), using data logging equipment.

## **TEST RESULTS**

### ***Mid-Span Deflections***

Figure 2 shows the total applied load versus mid-span deflection relationship for all the test beams. At the early stages of loading, all beams showed very similar stiffnesses, i.e. deformation due to load. At the post cracking stage of the concrete, beam E3, which was strengthened at the mid-span soffit, exhibited higher stiffness than those strengthened over the central support only (E2 and E5). As expected, beam E4 strengthened at the mid-span soffit and over the central support had the greatest stiffness of all the beams.

### ***End support reactions***

Figure 3 shows the amount of the load transferred to the end support plotted against the total applied load. As the results recorded for the two end support reactions were similar, only one end-support reaction is plotted in Figure 3. The end support at the beam failure,  $R$ , is also presented in Table 4. At the early stages of loading, the end support reactions of all the beams tested were very similar and were close to that obtained from an elastic analysis. Beams E1 and E4, which had nearly uniform flexural stiffness along the beam length, exhibited closer end support reactions to that obtained from linear elastic analysis up to failure. For the beams strengthened with CFRP laminates over the central support

only (beams E2 and E5), their end support reactions were less than that of the control beam E1 as the CFRP plate increases the flexural stiffness of the hogging zone. On the other hand, the end support reaction of beam E3, which had CFRP plate at the beam soffit, was higher than that of the control beam E1. The end support reactions of beams E2 and E5 strengthened with CFRP plate and sheets of equivalent tensile strength, respectively, were very similar.

### ***Modes and loads of failure***

The control beam E1 failed in a conventional ductile flexural failure mode due to yielding of the internal steel bars in tension followed by crushing of concrete in compression over the central support and then the mid-span sections as shown in Figure 4. The other four strengthened beams failed as a result of a peeling failure of the concrete cover adjacent to the external CFRP reinforcement as shown in Figures 5 (beam E3), 6 (beam E4) and 7 (beam E5). The peeling failure mode was brittle, sudden and explosive. In general, peeling failure of the CFRP laminate bonded over the central support was more explosive than that occurred for the soffit CFRP laminates. Peeling failure of the concrete cover occurred away from the CFRP laminate end in all beams apart from the soffit plates in beam E4 where the soffit plates failed due to plate separation without concrete attached. Peeling failure of the concrete cover in beam E3 was in the mid-span region on the side near the central support where there was high shear force. Extending the CFRP composite to cover the entire hogging zone, such as in beams E2, E4 and E5, or the entire sagging zone, such as in beams E3 and E4, did not prevent brittle separation of the CFRP laminates. The peeling failure, which occurred for the continuous beam tested in this experimental investigation is similar to that observed for simply supported beams tested elsewhere<sup>1,3,5,6</sup>.

Table 4 summarises the total failure load  $P_f$  (the sum of the two mid-span point loads) and



the ultimate load enhancement ratio ( $\xi$ ) which is the ratio of the ultimate load of an externally strengthened beam to that of the control beam. Strengthening the mid-span soffit (beam E3) was found to give a higher ultimate load enhancement ratio than strengthening the top of the beam over the central support (beams E2 and E5). Beam E4 strengthened with central support and mid-span CFRP plates failed at the highest load capacity and therefore showed the largest load enhancement ratio of all the strengthened beams tested. Using CFRP sheets of equivalent total tensile load capacity to the CFRP plates produced nearly the same load capacity (beams E2 and E5).

### ***Moment enhancement***

Figure 8 shows the total applied load plotted against the hogging and sagging bending moments for the beams tested. The bending moment was calculated from the equilibrium considerations of the beams using the measured end support reaction and mid-span applied load. The behaviour of all beams at low load levels was essentially elastic. As the applied load was increased, many cracks occurred, the steel reinforcement yielded and consequently the bending moment tended to become non-linear. Sagging bending moments of beams strengthened at mid-span soffit (such as E3) and hogging bending moment of beams strengthened over the central support (such as E2 and E5) were both higher than that calculated from elastic analysis.

Table 4 presents the ultimate moment enhancement ratio,  $\eta$ , which is the ratio of the ultimate moment of strengthened sections (hogging or sagging sections) to that of unstrengthened sections. In general, all the strengthened sections resisted a higher moment than the corresponding unstrengthened sections of the control beam. The ultimate moment enhancement ratio of beam E2 is nearly the same as that of beam E5 which was strengthened with CFRP sheets of equivalent strength to that of E2 plate. The ultimate moment enhancement ratio for strengthened sections is nearly the same as

(beam E4) or higher than (beams E2, E3, E5) the ultimate load enhancement ratio. The ultimate moment of all the strengthened sections is increased by approximately 50% of the original (control) moment capacity.

### ***Internal reinforcement strains***

Figure 9 presents the total applied load plotted against the tensile strains in the top steel bars over the central support and bottom steel bars at mid-spans. The yield load of the internal steel bars of the strengthened beams, that is the value of the applied load at which yielding of steel reinforcement occurred, is increased when compared with that of the corresponding control beam. The yield load of the tensile steel bars was governed by the position of the external CFRP composites. Where external CFRP laminates were provided, they carried tensile stresses which reduced stresses in the internal steel bars. For example, the yield load of the top steel bars over the central support is similar to that of the bottom steel bars at mid-spans for beams E1 and E4, but the yield load of the top steel bars over the central support is higher than that of the bottom steel bars at mid-spans for beams E2 and E5. Alternatively, the yield load of the bottom steel bars at mid-spans is higher than that of the top steel bars over the central support for beam E3. E2 steel strains in the top bars over the central support and bottom bars at mid-spans were very similar to those of E5. Although all steel bars yielded, failure of the strengthened beams mainly occurred due to peeling of the concrete cover attached to the CFRP laminates.

### ***CFRP laminate strains***

Figure 10 shows the total applied load plotted against the tensile strains measured at the middle of the CFRP composite for the strengthened beams. The strain gauge at the middle of the soffit CFRP plate in beam E4 was damaged during the early stages of loading, therefore it is not displayed in Figure 10.

The tensile strains of the CFRP composite increased significantly after concrete cracking and yielding of the internal tensile steel reinforcement. At loads higher than 80kN, the tensile strains in the CFRP sheets of beam E5 were higher than those measured in the CFRP plate of beam E2 as depicted in Figure 10, indicating initiation of bond slip between the sheets and concrete. Up to the yielding of the tensile steel reinforcement adjacent to the top central support CFRP plates in beams E2 and E4, the strains in the CFRP plates were the same as shown in Figure 10. Beyond yielding of the tensile steel reinforcement, beam E4 exhibited smaller strain in the CFRP plate over the central support than that observed in the CFRP plate of beam E2 at the same value of the applied load.

### ***Beam ductility***

Ductility of a structural element can be defined as its ability to sustain large deformations before reaching its failure. Two measures for the ductility of strengthened beams with FRP composites, namely deflection and energy ductility indices were adopted in the current investigation<sup>11-13</sup> as follows:

$$\mu_{\Delta} = \frac{\Delta_u}{\Delta_y} \quad (1)$$

$$\mu_E = \frac{E_u}{E_y} \quad (2)$$

where  $\mu_{\Delta}$  and  $\mu_E$  are the deflection and energy ductility indices, respectively,  $\Delta_u$  and  $E_u$  are the mid-span deflection and area under the load-deflection curve, respectively, at ultimate load and  $\Delta_y$  and  $E_y$  are the corresponding values at yield load of the tensile steel reinforcement. Table 5 gives these two ductility indices for the beams tested calculated at yielding of both sagging and hogging reinforcement. Although all the strengthened beams tested showed higher beam capacity than that of the control beam, the ductility of the strengthened beams was less than that calculated for the control beam.

Strengthening the hogging and sagging zones of beam E4 produced the least ductility of all strengthened beams tested. Beam E5 strengthened with CFRP sheets had less ductility than that calculated for beam E2 strengthened with CFRP plate as indicated in Table 5.

## **INTERFACE SHEAR STRESSES AT THE EXTERNAL PLATE END**

Several analytical methods have been developed for predicting peeling failure of reinforced concrete beams strengthened with external plates. These methods, however, were found to be derived for simply supported beams strengthened with external reinforcement and, therefore, are not directly applicable to continuous beams. As elastic theory has been widely used by a large number of researchers such as Jones et al.<sup>14</sup> Mukhopadhyaya and Swamy<sup>15</sup> and the Concrete Society<sup>7</sup>, it is applied to the beams tested in order to estimate interface shear stresses between the adhesive/concrete at failure.

### **Elastic Theory**

The force in the external plate at any two arbitrary sections (say 1-1 and 2-2 shown in Fig. 11) within the shear span can be determined from equilibrium consideration of each section. Then, the longitudinal shear stress at the adhesive level,  $\tau$ , is calculated by dividing the difference between the forces in the plate at the two sections by the product of the plate width and the distance between the two sections. Due to the smaller stiffness of the adhesive layer than the external plate, the shear stresses resulted from the variation of the force in the adhesive layer can be ignored<sup>15</sup>. Therefore, shear stresses at the adhesive/concrete interface can be taken the same as that at the plate/adhesive interface that has been referred to as the shear stresses  $\tau$  at the adhesive level. These stresses can also be calculated according to elastic theory from Eq. (3) below:

$$\tau = \frac{Qn_f t_f y_f}{I_c} \quad (3)$$

where  $\tau$  is the shear stress along the adhesive layer;  $Q$  is the shear force at the plate end calculated at beam failure;  $n_f$  is the external plate modular ratio ( $= E_f / E_c$  where  $E_f$  and  $E_c$  are the elastic moduli of the external plate and concrete, respectively);  $t_f$  is the thickness of the external plate;  $y_f$  is the depth of the external plate measured from the neutral axis to the centroid of the plate and  $I_c$  is the transformed second moment of area of the cracked plated reinforced concrete cross-section in terms of concrete.

The peak interface shear stresses  $\tau$  at the CFRP composite end calculated at the experimental failure load are given in Table 4. The calculated peak shear stresses at the plate end were close to the 0.80 N/mm<sup>2</sup> upper limit for shear stresses proposed in the Concrete Society Technical Report 55<sup>7</sup>. In other words, when the elastic shear stresses along the adhesive level are found to exceed 0.80 N/mm<sup>2</sup>, peeling failure would be expected to occur.

## CONCLUSIONS

Based on the limited test data presented in this paper, the following conclusions are drawn:

- Externally bonded CFRP laminates is an effective method of strengthening reinforced concrete continuous beams. The load and moment capacities were increased by up to 55% and 63%, respectively. However, the ductility of the strengthened beams is reduced.
- Peeling failure of the concrete cover adjacent to the CFRP composites was the dominant mode of failure for all the strengthened beams tested.
- Strengthening the mid-span soffit resulted in an increase in the end support reaction

compared with that of the control beam. Conversely, the end support reaction of beams strengthened at the hogging zone over the central support was less than that of the control beam.

- As expected, strengthening reinforced concrete continuous beams resulted in a reduction in the stresses in the steel bars at the strengthened sections compared with those in the control beam.
- The performance of the beams strengthened with plates or sheets of equivalent strength was similar.
- Beams with mid-span soffit CFRP reinforcement had a higher load capacity than those with central support strengthening.
- Mid-span soffit and central support strengthening was found to be the most effective arrangement to give the highest stiffness and load capacity.
- While the ultimate load and moment enhancement ratios are always the same for strengthened simply supported beams, the latter for strengthened sections is higher than the former.
- The calculated elastic interface shear stresses at beam failure were close to the upper limit recommended in the Concrete Society Technical Report 55.

## **ACKNOWLEDGEMENT**

The experimental work described in this paper was conducted in the Heavy Structures Laboratory in the University of Bradford; the assistance of the laboratory staff is acknowledged. The authors are grateful to Weber and Broutin (UK) Ltd. for providing the CFRP reinforcement and the associated priming and bonding materials for the research.

## REFERENCES

1. Arduini, M., Di Tommaso, A. and Nanni, A., "Brittle Failure in FRP Plate and Sheet Bonded Beams," *ACI Structural Journal*, Vol. 94, No. 4, July-August 1997, pp.363-370.
2. Ross, C. A., Jerome, D. M., Tedesco, J. W. and Hughes, M. L., "Strengthening of reinforced concrete beams with externally bonded composite laminates," *ACI Structural Journal*, Vol. 96, No 2, March-April 1999, pp. 212-220.
3. Saadatmanesh, H. and Ehsani, M. R., "RC beams strengthened with GFRP plates. I: Experimental study", *Journal of Structural Engineering*, ASCE, Nov. 1991, Vol. 117, No. 11, pp. 3417-3433.
4. Swamy, R. N., Mukhopadhyaya, P. and Lynsdale, C. J., "Strengthening for shear of RC beams by external plate bonding," *The Structural Engineer*, London, Vol. 77, No. 12, June 1999, pp.19-30.
5. Garden, H. N., Hollaway, L. C. and Thorne, A. M. "Preliminary evaluation of carbon fibre reinforced polymer plates for strengthening reinforced concrete members", *Proceedings of the Institution of Civil Engineers, Structures and Buildings Journal*, May, 1997, pp. 127-142.
6. Garden, H. N. and Hollaway, L. C. "An experimental study of the influence of plate end anchorage of carbon fibre composite plates used to strengthen reinforced concrete beams", *Composite Structures*, Vol. 42, 1998, pp. 175-188.
7. The Concrete Society Committee "Design guidelines for strengthening concrete structures using fibre composite materials", *The Concrete Society Technical Report 55*, Crowthorne, UK, 2001, 71 pp.
8. El-Refaie S. A., Ashour A. F., and Garrity S. W. "Tests of Reinforced Concrete Continuous Beams Strengthened with Carbon Fibre Sheets," *Proceedings of the*

- 10th BCA Annual Conference on Higher Education and Concrete Industry, Birmingham, UK, 29-30 June 2000, pp187-198.
9. Grace, N. F., Soliman, A. K., Abdel-Sayed, G. and Saleh, K. R. "Strengthening of continuous beams using fiber reinforced polymer laminates", Fourth International Symposium on Fiber Reinforced Polymer Reinforcement for Reinforced Concrete Structures, American Concrete Institute, 1999, pp. 647-657.
  10. Khalifa, A., Tumialan, G., Nanni, A. and Belarbi, A. "Shear strengthening of continuous reinforced beams using externally bonded carbon fiber reinforced polymer sheets", Fourth International Symposium on Fiber Reinforced Polymer Reinforcement for Reinforced Concrete Structures, American Concrete Institute, 1999, pp. 995-1008.
  11. Swamy, R. N., Lynsdale, C. J. and Mukhopadhyaya, P. "Effective Strengthening with Ductility: Use of Externally Bonded Plates of Non-metallic Composite Materials", 2<sup>nd</sup> International Conference on Advanced Composite Materials in Bridges and Structures, The Canadian Society for Civil Engineering, Montreal, Canada, 1996, pp. 481-488.
  12. Mufti, A. A., Newhook, J. P. and Tadros, G. "Deformability Versus Ductility in Concrete Beams with FRP Reinforcement", Advanced Composite Materials in Bridges and Structures, Canadian Society for Civil Engineering, 1996, pp. 189-199.
  13. Spadea, G., Bencardino, F. and Swamy, R. N. "Structural Behaviour of Composite RC Beams with Externally Bonded CFRP", Journal of Composites for Construction, August 1998, pp. 132-137.
  14. Jones, R., Swamy, R. N. and Charif, A. "Plate separation and anchorage of reinforced concrete beams strengthened by epoxy-bonded steel plates", *The*



*Structural Engineer*, The Institution of Structural Engineers, London, March 1988, Vol. 66, No. 5/1, pp. 85-94.

15. Mukhopadhyaya, P. and Swamy, N. "Interface shear stress: a new design criterion for plate debonding", *Journal of Composites for Construction*, ASCE, February 2001, pp. 35-43.
16. British Standards Institution "Testing concrete. Recommendations for the assessment of concrete strength by near-to-surface tests", BS 1881-207, Milton Keynes, UK, 1992.

## NOTATIONS

- $E_c$  = elastic modulus of concrete;
- $E_f$  = elastic modulus of CFRP plate;
- $E_s$  = Elastic modulus of steel reinforcement;
- $E_u$  = area under the load-deflection curve at ultimate load;
- $E_y$  = area under the load-deflection curve at yield load of the tensile steel reinforcement;
- $f_{cu}$  = cube strength of concrete;
- $f_r$  = modulus of rupture of concrete;
- $f_y$  = yield strength of steel reinforcement;
- $I_c$  = transformed second moment of area of the cracked plated reinforced concrete cross-section in terms of concrete.
- $n_f$  = external plate modular ratio;
- $P_t$  = total ultimate load of test specimens;
- $Q$  = shear force at the plate end calculated at beam failure;
- $y_f$  = depth of the external plate measured from the neutral axis to the centroid of the plate;
- $\xi$  = ultimate load enhancement ratio;
- $\eta$  = ultimate moment enhancement ratio;
- $\mu_\Delta$  = deflection ductility index;
- $\mu_E$  = energy ductility index;
- $\Delta_u$  = mid-span deflection at ultimate load;
- $\Delta_y$  = mid-span deflection at yield load of the tensile steel reinforcement;
- $\tau$  = interface shear stresses along the adhesive layer;

TABLE 1 Details of CFRP laminates used in the test specimens

Beam No.	Type	Size of CFRP laminates		Bonding adhesive used
		Top over the central support	Soffit at mid-spans	
E1	none	none	none	none
E2	plate	2500mm long x 100mm wide x 1.2mm thick	none	Epoxy structural adhesive
E3	plate	none	3500mm long x 100mm wide x 1.2mm thick	
E4	plate	2500mm long x 100mm wide x 1.2mm thick	3500mm long x 100mm wide x 1.2mm thick	
E5	Sheet	6 layers of 0.702mm total thickness x 110mm wide x 2500mm long	none	Epoxy bonding adhesive

TABLE 2 Properties of concrete and steel reinforcement used in the test specimens

Beam No.	Concrete		Internal steel reinforcement					
	$f_{cu}$ N/mm <sup>2</sup>	$f_r$ N/mm <sup>2</sup>	16mm dia. Longitudinal bars			Vertical stirrups		
			No.	$f_y$ N/mm <sup>2</sup>	$E_s$ kN/mm <sup>2</sup>	No.	$f_y$ N/mm <sup>2</sup>	$E_s$ kN/mm <sup>2</sup>
E1	24.0	3.0	2 bars (top) + 2 bars (bottom)	520	201	6mm closed links at 100mm centres	308	200
E2	43.6	4.6						
E3	47.8	4.4						
E4	46.1	4.4						
E5	44.7	4.8						

Table 3 Properties of strengthening materials

Material property	Primer	Bonding adhesive	Structural adhesive	CFRP sheet	CFRP plate
Compressive strength (N/mm <sup>2</sup> )	100	80	85	N/A	N/A
Tensile strength (N/mm <sup>2</sup> )	19	17	19	3900	2500
Young's Modulus (kN/mm <sup>2</sup> )	5.0	5.0	9.8	240	150
Flexural strength (N/mm <sup>2</sup> )	30	28	35	N/A	N/A
Bond to concrete (N/mm <sup>2</sup> )	5.3	4.0	20.0	N/A	N/A

TABLE 4 Test results at failure of test specimens

Beam No.	$P_t$ (kN)	$R$ (kN)	$\xi$	$\eta$		$\tau$ (N/mm <sup>2</sup> )	Failure mode
				sagging	hogging		
E1	149.67	23.19	1.00	1.00	1.00	N/A	Flexural mode
E2	178.64	23.38	1.19	1.00	1.52	0.802	Peeling failure
E3	207.06	37.78	1.38	1.57	1.05	0.816	Peeling failure
E4	231.42	37.75	1.55	1.57	1.51	0.967* 0.749**	Peeling failure
E5	174.58	23.43	1.17	0.99	1.48	0.789	Peeling failure

\* Shear stresses at the end of the top plate.

\*\* Shear stresses at the end of the bottom plate.

$P_t$  =ultimate load;  $R$  = end support reaction at failure;  $\xi$  = ultimate load enhancement ratio;  $\eta$ = ultimate moment enhancement ratio;  $\tau$  = peak shear stresses at the concrete/adhesive interface calculated at beam failure

Table 5 Deflection ductility index ( $\mu_{\Delta}$ ) and energy ductility index ( $\mu_E$ ) of beams tested

Beam no.	$\mu_{\Delta}$		$\mu_E$	
	sagging	hogging	sagging	hogging
E1	5.40	6.12	11.10	14.30
E2	3.58	2.48	6.96	3.85
E3	2.18	3.21	3.32	6.21
E4	1.91	2.10	2.92	3.43
E5	2.60	2.02	4.89	3.14

**Biographical Sketch:**

**S.A.El-Refaie** is currently a lecturer at Helwan University, Egypt. He obtained his BSc degree from the Department of Civil Engineering, Helwan University, Egypt in 1994 and his PhD from the Department of Civil & Environmental Engineering at the University of Bradford, UK in 2001.

**A.F.Ashour** is currently a lecturer at the University of Bradford, UK. He obtained his BSc and MSc degrees from Mansoura University, Egypt and his PhD from Cambridge University, UK. His research interests include shear, plasticity and optimisation of reinforced concrete and masonry structures.

**S. W. Garrity** is a visiting research fellow at the University of Bradford, UK and the principal of Garrity Associates.





Figure 5 Plate separation of CFRP laminates at soffit mid span (beam E3)





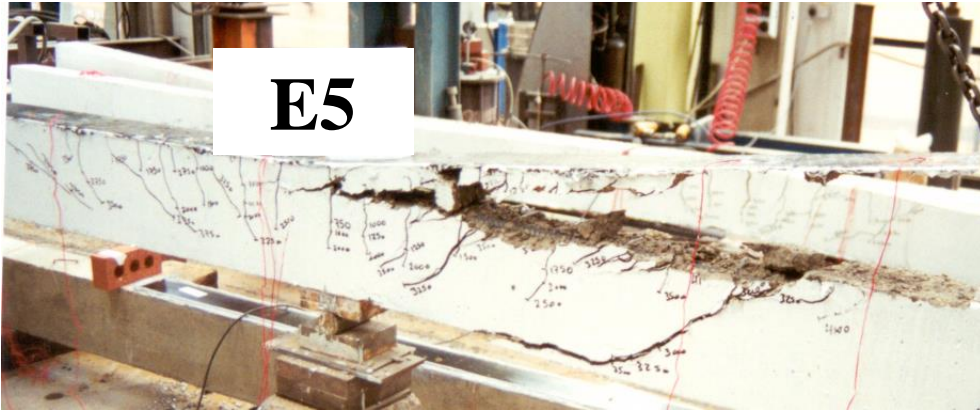


Figure 7 Peeling failure of CFRP sheets over the central support of beam E5

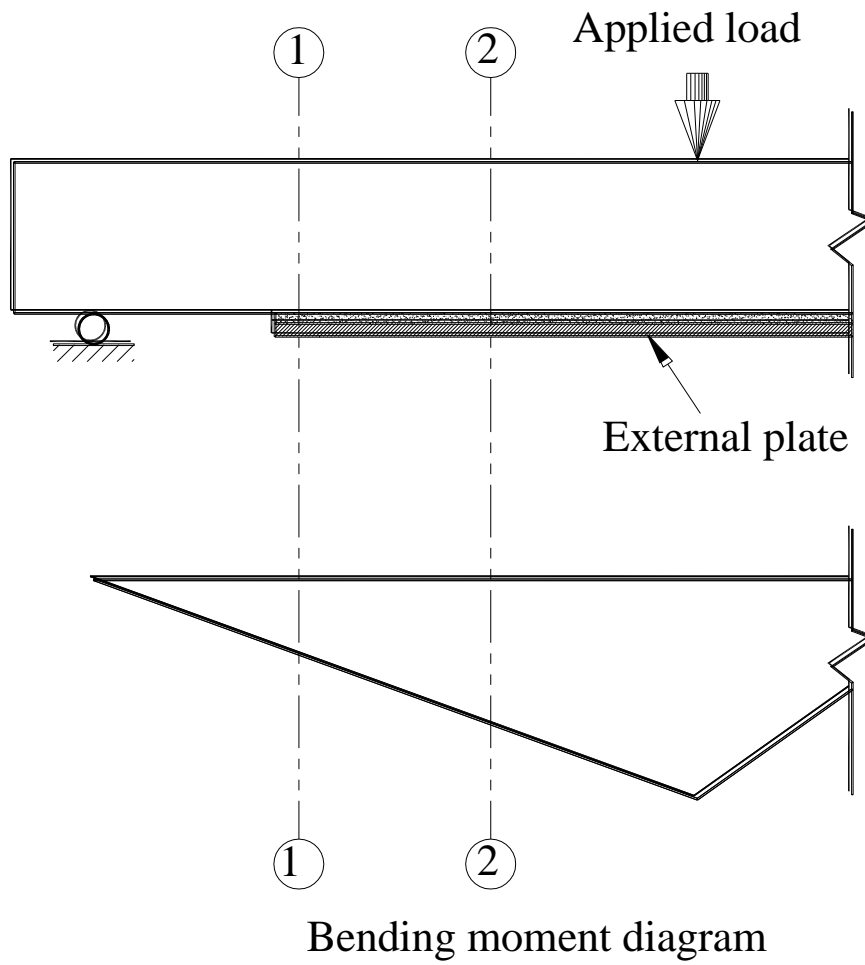


Figure 11 Two arbitrary sections along the plate length in the shear span.